RIGI: Rectifying Image-to-3D Generation Inconsistency via Uncertainty-aware Learning

Jiacheng Wang[1], Zhedong Zheng[2], Wei Xu[1†], Ping Liu[3†]

[1]EIC, Huazhong University of Science and Technology
[2]FST and ICI, University of Macau
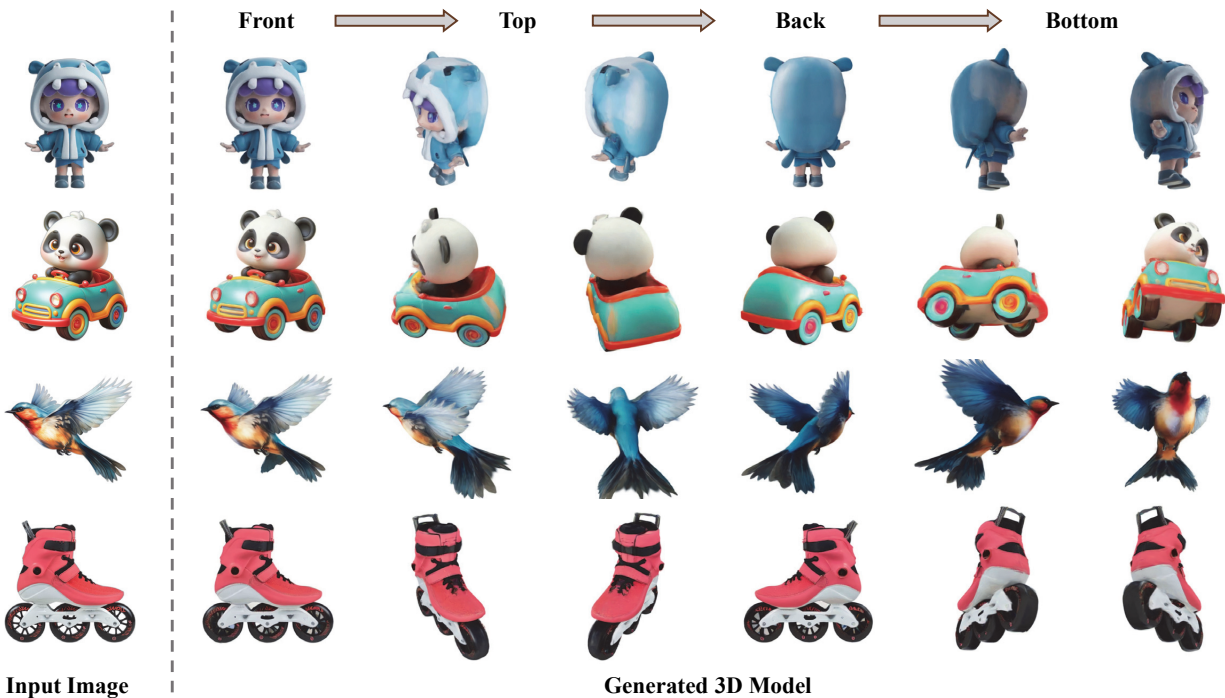[3]CSE, University of Nevada, Reno

Figure 1. Given an input image, our method mitigates the impact of inconsistencies between generated dense frames on 3D asset optimization, reducing edge artifacts and floats while producing visually impressive 3D objects. We sample six rendered images uniformly across an azimuth range of 0 to 360°, with elevations following a sine function with a 30° amplitude, effectively capturing **front, top, back, and bottom** perspectives, which are crucial to real-world applications, yet often overlooked by most existing methods.

Abstract

Given a single image of a target object, image-to-3D generation aims to reconstruct its texture and geometric shape. Recent methods often utilize intermediate media, such as multi-view images or videos, to bridge the gap between input image and the 3D target, thereby guiding the generation of both shape and texture. However, inconsistencies in the generated multi-view snapshots frequently introduce noise and artifacts along object boundaries, undermining the 3D reconstruction process. To address this challenge, we lever-age 3D Gaussian Splatting (3DGS) for 3D reconstruction, and explicitly integrate uncertainty-aware learning into the reconstruction process. By capturing the stochasticity between two Gaussian models, we estimate an uncertainty map, which is subsequently used for uncertainty-aware regularization to rectify the impact of inconsistencies. Specifically, we optimize both Gaussian models simultaneously, calculating the uncertainty map by evaluating the discrepancies between rendered images from identical viewpoints. Based on the uncertainty map, we apply adaptive pixel-wise loss weighting to regularize the models, reducing reconstruction intensity in high-uncertainty regions. This ap-

† denotes corresponding authors.

1

proach dynamically detects and mitigates conflicts in multi-view labels, leading to smoother results and effectively reducing artifacts. Extensive experiments show the effectiveness of our method in improving 3D generation quality by reducing inconsistencies and artifacts. More visual results can be found here.

1. Introduction

Image-to-3D generation aims to create 3D objects with corresponding shapes and textures from a single-view image, significantly reducing manual modeling costs and accelerating 3D creation. Recent advancements in diffusion models [2, 40, 42] have led to approaches [26, 27, 37, 38, 64] that leverage the generative capabilities of pre-trained 2D diffusion models for 3D generation. However, these 2D diffusion models lack intrinsic 3D perception, often resulting in geometric inconsistencies between generated views. This limitation compromises the accuracy of the resulting 3D assets, particularly when handling multiple perspectives.

To achieve high consistency in image-to-3D generation, recent research has focused on modifying diffusion models to improve geometric alignment across multi-view images. For instance, one line of methods [24, 28, 46, 47, 57, 60] applies global self-attention to integrate multi-view information, but this increases computational costs, limiting both image resolution and the number of feasible viewpoints. Alternatively, another line of methods [6, 30, 55, 63, 74] employs video diffusion models to maintain spatio-temporal consistency, enabling high-resolution, spatially coherent frames that are then optimized into high-quality 3D assets through a reconstruction-based approach.

Despite these advancements, inconsistencies between generated frames still pose significant challenges, introducing artifacts and errors in the 3D generation process, which is illustrated in Figure 2. Pseudo-labels from different viewpoints may exhibit varying geometric structures or textural details within the same 3D region, causing conflicts during subsequent optimization.

To address these issues, we introduce uncertainty-aware learning into the optimization process of 3D assets. Given its efficient training and high-quality rendering, we use 3DGS [19] as our 3D representation. Our approach consists of two key steps: uncertainty estimation and uncertainty regularization. In the first step, we simultaneously optimize two Gaussian models and model uncertainty by capturing the stochastic differences between them. The uncertainty map is estimated by calculating the absolute difference between the rendered images of the two models. In the second step, we conduct uncertainty regularization based on the estimated uncertainty map. This step dynamically adjusts pixel-wise loss weights, reducing the impact of inconsistent pseudo-labels in high-uncertain regions. Our
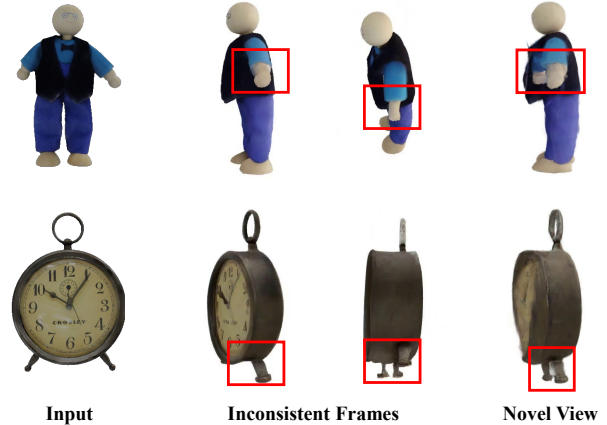

Figure 2. Prevailing Image-to-3D methods typically adopt the synthesized video as an intermediate representation to guide the 3D object generation. However, the frame-to-frame inconsistencies can lead to incorrect geometry and artifacts in the 3D assets. In this example, red bounding boxes highlight extra toy arms and clock legs, which represent common failures in the generation process.

approach dynamically detects pseudo-label inconsistencies during optimization and progressively alleviates their negative impact on 3D assets generation. Extensive experiments show that it mitigates artifacts and improves 3D generation quality both quantitatively and qualitatively. In summary, our contributions are as follows:

- We introduce uncertainty-aware learning into 3D Gaussian Splatting, modeling the uncertainty between generated pseudo-labels by leveraging the variations between two concurrently optimized Gaussian models. We apply uncertainty regularization based on estimated uncertainty maps to mitigate conflicts in generated pseudo-frames.
- Extensive experiments show that our approach, combined with a multi-view video diffusion model, produces 3D assets of high quality, as evidenced by both quantitative and qualitative analyses.

2. Related Work

Image-to-3D Generation. Image-to-3D generation aims to create accurate 3D assets from a single 2D image, a challenging task requiring reliable modeling of unseen views. Early methods focused primarily on single-view 3D reconstruction [8, 31, 54, 56, 71], while recent advancements have shifted towards employing image-based 3D generative models with diverse 3D representations [11, 16, 34, 58, 61], enabling the generation of more complex 3D assets.

While traditional 3D generation methods require high-quality 3D data, limiting their generalization, large-scale 2D diffusion models [2, 40, 42] have shown success in generating high-quality images and videos, inspiring 2D-to-3D lifting approaches. DreamFusion [37] and Zero123 [27]

leverage pre-trained 2D diffusion models to optimize 3D assets and synthesize new views, demonstrating strong 3D consistency. However, these methods remain computationally expensive. To address this, recent research has focused on more efficient feed-forward approaches, particularly large reconstruction models (LRMs) [4, 13, 53], which map image features into 3D triplane space for faster 3D asset creation. Subsequent works [24, 28, 46, 47, 57, 60, 65] have integrated multi-view diffusion models, improving both geometry and texture quality. The methods leveraging temporal consistency in video models [6, 30, 55, 63, 74] enhance 3D reconstruction by first generating dense video frames and then performing 3D reconstruction.

In this paper, we follow a two-stage approach that yields visually impressive results with detailed textures, leveraging the ability of video models to generate dense and high-quality frames. However, the multi-view frames generated by these methods often exhibit inconsistencies in both geometry and texture. Addressing the impact of these inconsistencies on subsequent 3D asset optimization remains an important challenge and the focus of our work.

Uncertainty-aware Learning. With the advancement of deep learning, there is a growing focus on improving the reliability and interpretability of the model. Estimating the model uncertainty not only improves the interpretability but also provides a quantitative measure of output confidence. Early work [18] categorizes uncertainty into two types, *i.e.*, epistemic uncertainty and aleatoric uncertainty. Epistemic uncertainty, also known as model uncertainty, refers to the variability in model weights trained on the same dataset. Pioneering methods such as Bayesian networks [33, 36], dropout [9, 20], and adding Gaussian noise [5, 66] exploit inherent randomness in neural networks to estimate this uncertainty, typically by modeling the variance in weight distributions. Other approaches [22, 32, 39, 69] explicitly model uncertainty through an auxiliary branch, though at the cost of higher training expenses and potential accuracy trade-offs. Aleatoric uncertainty, on the other hand, represents noise in observations, including both input data and annotations. Many approaches [18, 25, 72] model aleatoric uncertainty to identify noise in inputs or annotations, using a dynamic uncertainty-aware loss to stabilize training and improve the final results.

Uncertainty estimation has been widely explored in the 3D domain, particularly within Neural Radiance Fields (NeRF) and 3D Gaussian Splatting (3DGS). Uncertainty in NeRF models arises from factors such as variations in camera models, lighting conditions [15, 41], occlusions, and sparse viewpoints [29, 44, 45]. Approaches such as Bayesian reparameterization [35, 44, 45] and volume rendering [62, 67] model uncertainty by quantifying the variability in weight distributions or density along rays. Fisher information has also been applied [10, 14] to quantify un-

certainty in rendered views.

Recently, 3DGS has garnered significant attention for its high-quality reconstruction and efficient rendering, incorporating uncertainty estimation to improve output confidence. Studies [21, 43] have investigated modeling uncertainty within 3DGS, facilitating effective quantification of output confidence and alleviating the impacts of noise, occlusion, and imprecise camera poses on the reconstruction process. Additionally, uncertainty information has been used for next-view selection [23, 49], optimizing the reconstruction process by identifying beneficial viewpoints, thus reducing the need for extensive scene capture. More recent works [50, 70] have integrated uncertainty-aware learning into training, dynamically adjusting pixel contributions to minimize noise in uncertain regions.

In this work, we tackle the challenging problem of Image-to-3D generation, focusing on mitigating noise and inconsistencies across synthesized multi-view frames. Our approach introduces a dynamic, uncertainty-aware mechanism that adapts pixel-wise loss weights based on the estimated uncertainty, enhancing the robustness of the generation process. This method significantly reduces visual artifacts and distortion in generated 3D assets.

3. Method

Our pipeline, as shown in Figure 3, takes a reference image as input and outputs 3D assets. We adopt a two-stage approach: first, a multi-view video diffusion model generates dense, high-quality frames, which serve as pseudo-labels to guide 3D asset optimization; second, uncertainty-aware learning is applied to optimize the 3D assets, improving robustness and reducing artifacts in the final output. In Section 3.1, we introduce 3D Gaussian Splatting and the video diffusion models that form the foundation of our approach. In Section 3.2 and 3.3, we describe the integration of uncertainty-aware learning into the 3D asset optimization process, encompassing both uncertainty estimation and regularization. Finally, in Section 3.4, we discuss additional optimization strategies used to further enhance visual quality throughout the optimization process.

3.1. Preliminary

3D Gaussian Splatting. 3DGS [19] is a point-based explicit 3D representation composed of a set of learnable Gaussian points. Each Gaussian point is parameterized by the center position $\mu_i \in \mathbb{R}^3$, scaling $s_i \in \mathbb{R}^3$, rotation $r_i \in \mathbb{R}^4$, color $c_i \in \mathbb{R}^3$, spherical harmonic (SH) coefficients $h_i \in \mathbb{R}^{3 \times (k+1)^2}$ up to order k, and opacity $\sigma_i \in \mathbb{R}$. The Gaussian model can be queried as:

$$G(x) = e^{-\frac{1}{2}(x-\mu)^\top \boldsymbol{\Sigma}^{-1}(x-\mu)}, \; \Sigma_i = R_i S_i S_i^T R_i^T, \quad (1)$$

where x is a given 3D position, $\boldsymbol{\Sigma}$ is the covariance matrix, S_i and R_i are the scaling and rotation matrices derived from
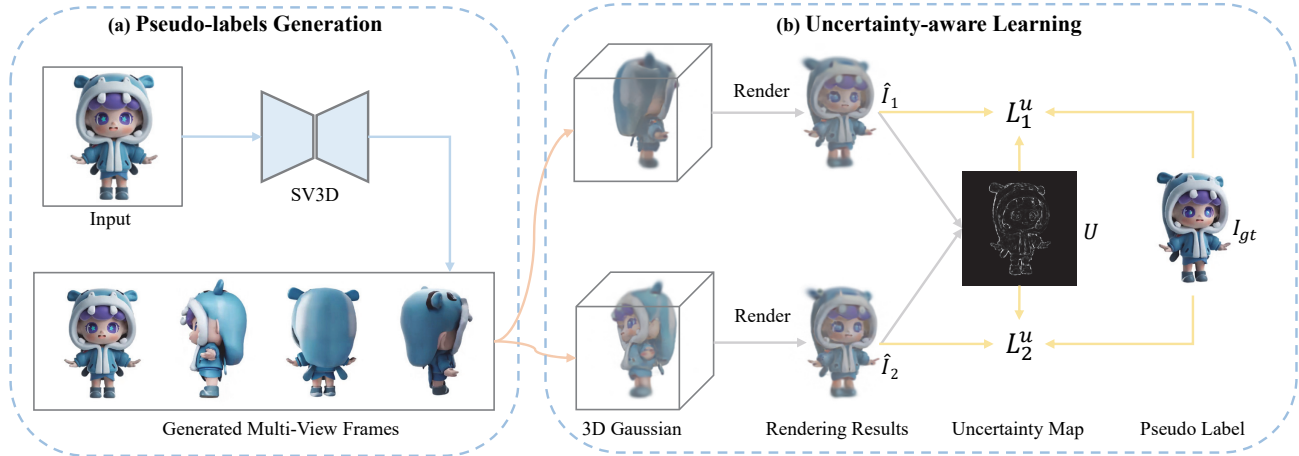
Figure 3. **Overview of our pipeline.** Firstly, we use SV3D [55] to generate multiple videos with a wide range of viewpoints, which serve as pseudo-labels for 3D asset optimization. Next, we introduce uncertainty-aware learning, estimating an uncertainty map by leveraging the stochasticity of two simultaneously optimized Gaussian models. Finally, we apply uncertainty-aware regularization to mitigate the impact of inconsistencies in the generated pseudo-labels, resulting in high-quality and visually impressive 3D assets.

s_i and r_i, respectively.

To render a 2D image from a specific camera pose, the color of each pixel is determined by α-blending of the sorted Gaussian points:

$$C = \sum_{i=1}^{N} c_i \alpha_i \prod_{j=1}^{i-1} (1 - \alpha_j), \qquad (2)$$

where c_i is the color and α_i represent the projected opacity.

The Gaussian model is trained using a reconstruction loss function: $\mathcal{L} = (1 - \lambda)\mathcal{L}_1 + \lambda\mathcal{L}_{\text{D-SSIM}}$, where λ is empirically set to 0.2. Starting from a sparse point cloud, the model applies a densification process that duplicates and splits high-gradient Gaussian points, complemented by a pruning strategy to eliminate non-essential points. In this work, we adopt 3DGS as our 3D representation due to its efficient training and high-quality rendering capabilities.

Video Diffusion Model. Video diffusion models [2, 3] are typically built upon pre-trained 2D image diffusion models [12, 40, 48], enabling the generation of spatially and temporally consistent video sequences by denoising multiple frames simultaneously. A representative approach is Stable Video Diffusion (SVD) [2], which consists of an encoder ε, a denoising U-Net ϵ_θ, and a decoder $\mathcal{D}$. SVD achieves high-quality and consistent video generation in recent works. Given a condition image c and an initial sequence of random noise x_T, the denoising U-Net estimates the added noise at timestep t. The noise scheduler [17] progressively removes noise at each timestep to produce x_{t-1}, which can be written as:

$$x_{t-1} = \Phi\left(\epsilon_\theta\left(x_t; t, c\right), t, x_t\right), \qquad (3)$$

where Φ denotes the noise scheduler and c represents the

condition embedding. After T denoising steps, a high-quality sequence of N video frames is generated.

Building on the spatiotemporal consistency of SVD, SV3D [55] adapts the denoising U-Net to condition on camera pose, offering precise control over viewpoints and improving multi-view consistency in image-to-3D generation:

$$x_{t-1} = \Phi\left(\epsilon_\theta\left(x_t; t, c, a, e\right), t, x_t\right), \qquad (4)$$

where a and e denote the azimuth and elevation angles, respectively. With an input image, SV3D can generate N frames from different viewpoints, supporting both static and dynamic camera orbits. In this study, we employ SV3D to generate multi-view frames as pseudo-labels for 3D assets optimization, leveraging its state-of-the-art performance in geometric and texture consistency, along with its ability to control dynamic camera poses.

3.2. Uncertainty Estimation

In Image-to-3D generation, uncertainty arises from two main sources: epistemic uncertainty, due to the limited information from a single image, and aleatoric uncertainty, due to inherent noise or inconsistencies in the input data. Epistemic uncertainty leads to variations in the 3D assets, particularly in unobserved regions, which is mitigated by using a multi-view video diffusion model to generate dense frames from multiple viewpoints. Aleatoric uncertainty results from visual overlaps between pseudo frames, introducing inconsistencies in geometry and texture that can cause artifacts during optimization process.

As discussed, uncertainty estimation is crucial for mitigating the impact of noisy pseudo-labels on 3D asset optimization. To estimate uncertainty, we model the discrepan-

4

cies between two simultaneously optimized Gaussian models. This approach leverages the inherent randomness in the training process: when optimized with the same data, 3D assets will naturally exhibit variations. These variations indicate the degree of uncertainty in the generated pseudo-labels. Specifically, regions with higher uncertainty will show greater variability, resulting in more pronounced differences between the models, while regions with lower uncertainty will exhibit less variation. By capturing these differences, we accurately estimate the inconsistency in the noisy labels, and in turn, guide the optimization process to improve the stability and accuracy of the 3D generation.

Specifically, given a set of generated multi-view labels $\mathcal{I}^{gt} = \{I_i^{gt}\}_{i=1}^M$ corresponding to various camera poses $\mathcal{P} = \{P_i\}_{i=1}^M$, we simultaneously optimize two Gaussian models, $\mathcal{G}_1$ and $\mathcal{G}_2$, where M denotes the number of frames. During each optimization step, we randomly sample a camera pose $P_i \in \mathcal{P}$, and render both Gaussian models from the corresponding viewpoint to obtain the rendered images $\hat{I}_1$ and $\hat{I}_2$. Then the uncertainty of the Gaussian models under a given camera pose is approximated by the difference between the rendered images $\hat{I}_1$ and $\hat{I}_2$:

$$U = |\hat{I}_1 - \hat{I}_2|. \tag{5}$$

Notably, each Gaussian model is randomly initialized, ensuring observable differences between $\mathcal{G}_1$ and $\mathcal{G}_2$ throughout the optimization. This variability enables the models to effectively capture and model the uncertainty in the pseudo-labels, guiding the optimization effectively.

Why not adopt a learnable approach to model uncertainty? For 3DGS, one approach to model uncertainty is to assign a learnable variance property to each Gaussian point, allowing an uncertainty map to be rendered through α-blending. During optimization, the variance parameter is dynamically updated. However, directly regressing the uncertainty in this manner may lead to training instability, as the variance of certain Gaussian points may become excessively large or small, hindering the achievement of an optimal result. In contrast, our approach avoids directly optimizing the variance. Instead, we model uncertainty by capturing the differences between two Gaussian models, which enhances optimization stability. Our experiments show that two Gaussian models are sufficient, and their absolute difference effectively captures uncertainty. Based on the estimated uncertainty map, uncertainty-aware regularization effectively mitigates artifacts and floats in 3D assets caused by inconsistencies in pseudo-labels.

3.3. Uncertainty Regularization

In Image-to-3D generation, inconsistencies in pseudo multi-view frames often cause issues during optimization, especially in regions with high uncertainty. The inconsistencies arise when pseudo-labels from different viewpoints

conflict, leading to conflicting optimization directions and artifacts or floats in the generated 3D assets. To address this, we adjust the pixel-wise loss by incorporating our estimated uncertainty map. Specifically, we modify the original loss function, which includes a pixel-wise loss term and a D-SSIM term, to account for these inconsistencies:

$$
\begin{aligned}
\mathcal{L}_1^u &= \frac{|I_{gt} - \hat{I}_1|}{\exp(\lambda \cdot U)} + \lambda \cdot U, \\
\mathcal{L}_2^u &= \frac{|I_{gt} - \hat{I}_2|}{\exp(\lambda \cdot U)} + \lambda \cdot U,
\end{aligned}
\tag{6}
$$

where U represents the uncertainty between the two Gaussian models, λ controls the strength of the uncertainty regularization. By dynamically adjusting the loss based on the uncertainty, we improve the stability and quality of the 3D asset generation, particularly in uncertain regions.

Notably, we amplify the estimated uncertainty map to increase the variation in regularization loss, using an experimentally determined factor $\lambda = 5$. The first term dynamically adjusts the optimization intensity for each pixel in the pseudo-labels, based on the estimated uncertainty map. Regions with higher inconsistencies receive lower weights, reducing their influence on the optimization process. The second term regularizes the uncertainty map, preventing excessive disparity between the two Gaussian models that could result in high uncertainty across all viewpoints. When the uncertainty map is constant at zero, the regularization term reduces to the standard L1 loss, where each region is optimized with a constant weight. Given the effectiveness of LPIPS loss [68] in enhancing visual quality, we incorporate it into the reconstruction loss. The LPIPS loss and the D-SSIM Loss [59] are then formulated as:

$$
\begin{aligned}
\mathcal{L}_{lpips} &= \text{LPIPS}(I_{gt}, \hat{I}_1) + \text{LPIPS}(I_{gt}, \hat{I}_2), \\
\mathcal{L}_{d\text{-}ssim} &= \text{D-SSIM}(I_{gt}, \hat{I}_1) + \text{D-SSIM}(I_{gt}, \hat{I}_2).
\end{aligned}
\tag{7}
$$

Finally, the total loss is given by:

$$\mathcal{L}_{total} = (1 - \lambda_s)(\mathcal{L}_1^u + \mathcal{L}_2^u) + \lambda_s \mathcal{L}_{d\text{-}ssim} + \lambda_l \mathcal{L}_{lpips}, \tag{8}$$

where λ_s and λ_l are empirically set to 0.2 and 0.5.

How does uncertainty regularization impact the optimization of 3D assets? Generated multi-view frames often exhibit inconsistencies in overlapping regions, where pseudo-labels from different viewpoints may conflict in their optimization directions. In such cases, Gaussian models may densify redundant points to satisfy the pseudo-labels from certain viewpoints, potentially leaving uncovered viewpoints vulnerable to artifacts or floats. By applying uncertainty regularization, regions with high inconsistency are assigned higher uncertainty values. This reduces the conflicting influence of pseudo-labels, diminishing the need to densify redundant Gaussian points and leading to a smoother outcome in inconsistent regions.

Table 1. **Quantitative Comparison.** Our method achieves superior or comparable results, demonstrating its effectiveness in generating high-quality 3D assets.

Methods	PSNR↑	SSIM↑	LPIPS↓
DreamGaussian [51]	17.162	0.8252	0.2039
TriplaneGaussian [73]	14.0062	0.8161	0.2531
LGM [52]	14.5874	0.8083	0.2488
V3D [6]	17.1847	0.8085	0.2055
Hi3D [63]	**17.2559**	0.8217	0.2014
Ours	16.9646	**0.8346**	**0.2003**

3.4. Optimization Strategy

To enhance the quality of 3D generation, we apply several optimization techniques along with uncertainty estimation and regularization. Specifically, we integrate Perturbed-Attention Guidance (PAG) [1] into the multi-view video diffusion model, improving texture and geometry, particularly in rear-view perspectives. Camera poses are sampled across a range of elevation and azimuth angles to ensure robust 3D asset generation from various viewpoints. For optimization, we use multi-scale rendering and progressive sampling strategies to balance training efficiency and visual quality. Initially, the optimization focuses on geometric structure, with progressive increases in resolution to capture finer texture details. We also progressively introduce frames with varying elevations to stabilize the training process and reduce inconsistencies in geometry initialization. Additionally, we mitigate redundant white Gaussian points in inconsistent regions by applying a random background color technique, effectively reducing white artifacts. These strategies enhance both reconstruction quality and visual consistency, resulting in more impressive 3D outputs.

4. Experiments

Implementation Details. For multi-view frames generation, we employ $sv3d\_p$ [55], which generates frames from various viewpoints along a dynamic orbit. We then sample multiple videos with azimuth angles uniformly distributed across 360°, and elevation angles defined by sinusoidal amplitudes of 0°, -20°, and 40°, resulting in 63 frames in total. For 3D asset optimization, we follow the original setup of 3DGS [19], with minor modifications. Specifically, the spherical harmonics (SH) degree is set to 0, and the total optimization iterations is reduced to 5000. During the optimization process, we progressively increase the render radio, beginning at 0.25 and scaling up to 0.5 at 20% of the total iterations, and reaching 1.0 at 50% of the total iterations. Additionally, we progressively incorporate frames with different elevations throughout the optimization process, at 50% and 80% of the total iterations, respectively. For the camera setup, the field of view (FOV) is configured

at 33.8° with a radius of 4.0.

Baselines. We selected five image-to-3D generation methods based on 3D Gaussian Splatting [19] for comparison: (1) **DreamGaussian** [51] is an optimization-based approach that refines 3D assets under the supervision of Zero123 [27]; (2) **TriplaneGaussian** [73] is an inference-only method that proposes a hybrid triplane-gaussian representation to achieve fast and high-quality 3D reconstruction; (3) **LGM** [52] is another inference-only method that reconstructs Gaussian models from generated multi-view images; (4) **V3D** [6] is a multi-view video diffusion model that generates dense frames, which are then used as pseudo-labels for 3D asset reconstruction; (5) **Hi3D** [63] employs a two-stage generation paradigm to produce high-resolution multi-view frames, enhancing the generated texture details.

Evaluation Metrics. To evaluate the visual quality of the generated assets, we selected 25 objects from the GSO dataset [7], manually choosing front-facing input images. We rendered 36 ground truth images with uniformly sampled azimuth angles and randomly sampled elevation angles, ensuring coverage of both top and bottom perspectives of the 3D assets. We then used PSNR, SSIM, and LPIPS as evaluation metrics to measure the difference between the generated views and the ground truth.

4.1. Experimental Results

Qualitative Results. As shown in Figure 4, we provide qualitative comparisons across several approaches, including optimization-based, inference-only, and two-stage methods. TriplaneGaussian [73], though efficient in generating 3D assets, yields lower-resolution outputs with limited texture detail. LGM [52] employs an asymmetric U-Net to produce high-resolution 3D objects; however, inconsistencies in the input multi-view images may result in artifacts and floats. DreamGaussian [51] leverages SDS Loss for 3D object optimization, but it often generates coarse textures on the back, leading to a disconnect between front and back views. V3D [6] and Hi3D [63] employ multi-view video diffusion models to generate dense, high-quality frames, producing 3D objects with detailed textures. However, since optimization is performed from a limited set of fixed viewpoints, these methods may overfit to the generated frames, resulting in underdeveloped geometry and texture details from top and bottom perspectives. Our approach samples videos from diverse viewpoints and uses uncertainty-aware learning to mitigate inconsistencies, resulting in visually impressive 3D outputs.

Quantitative Results. We selected 25 objects from the GSO [7] dataset and used SSIM, PSNR, and LPIPS to evaluate the visual quality of the generated 3D objects. As shown in Table 1, we achieve superior or comparable results, demonstrating the effectiveness of our approach in generating high-quality and visually impressive 3D assets.
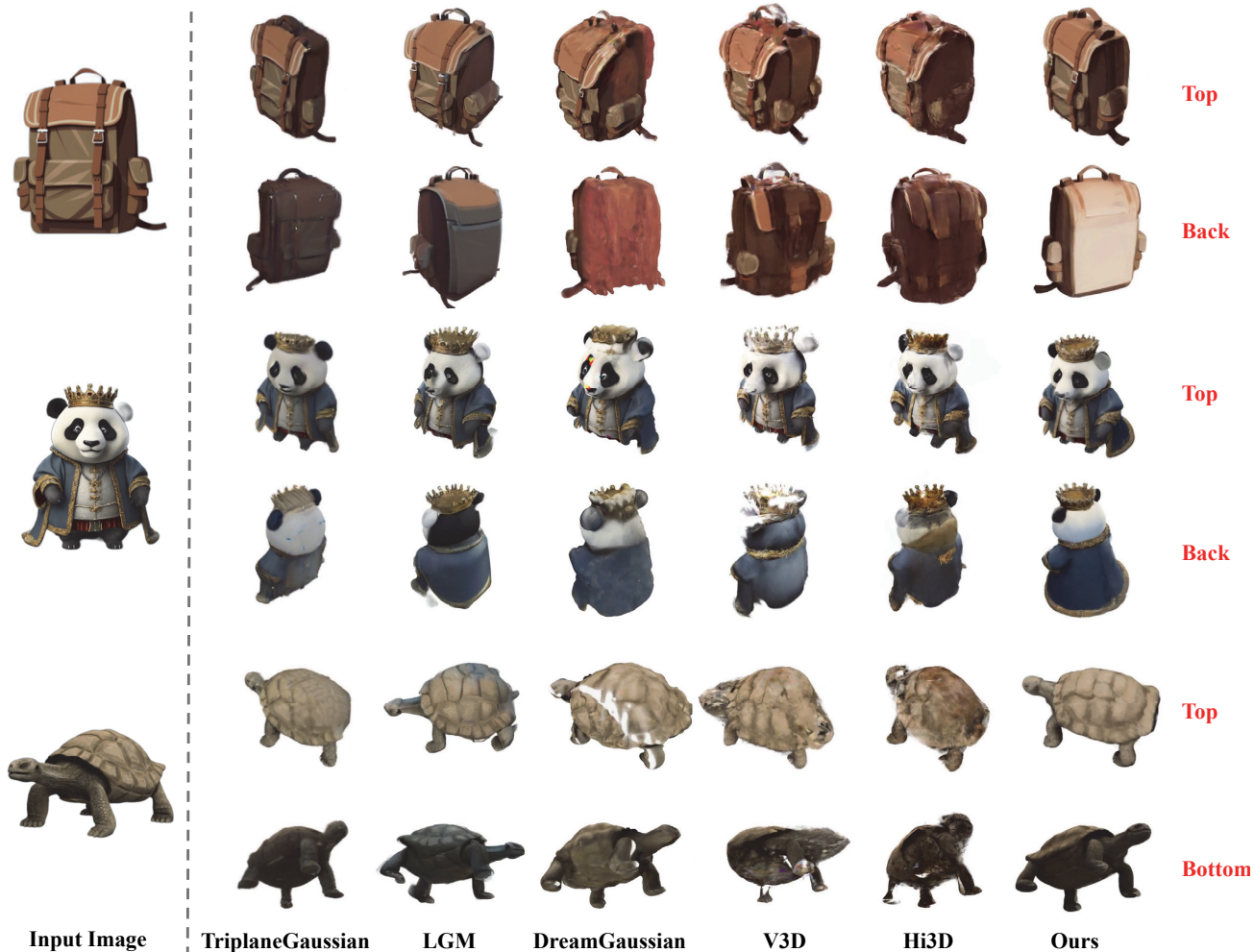
Figure 4. **Visual Comparison**. Here we compare competitive image-to-3D methods, including TriplaneGaussian [73], LGM [52], Dream-gaussian [51], V3D [6] and Hi3D [63]. We achieve visually impressive results, with high-quality geometric and texture details even from top and bottom perspectives.

Table 2. **User Study**. We curate a set of 30 samples and conduct a user study with 35 participants, each tasked with selecting the top two results that best matched the input image and exhibited the highest visual quality. Our method achieved the highest preference score, demonstrating its capability to produce visually compelling 3D assets.

Methods	TriplaneGaussian [73]	LGM [52]	DreamGaussian [51]	V3D [6]	Hi3D [63]	Ours
Preference↑	19.81%	46.95%	25.14%	19.24%	21.91%	**66.95%**

Specifically, our method performs well on SSIM, indicating excellent structural consistency and effectively mitigating noise, artifacts, and floats in inconsistent areas. Additionally, we observe a slight improvement in LPIPS, suggesting good perceptual quality in the generated 3D assets. However, we did not achieve the highest PSNR score, slightly trailing behind Hi3D [63], which may seem inconsistent with the qualitative results. We hypothesize that uncertainty regularization dynamically adjusts pixel-level supervision

in the pseudo-labels, prioritizing structural smoothness in inconsistent regions rather than redundant Gaussian points for pixel-level alignment. Consequently, this approach may yield slightly lower scores on pixel-wise metrics, which tend to favor precise structural coherence.

User Study. To evaluate visual quality, we curated a set of 30 samples and conducted a user study with 35 participants, as summarized in Table 2. Each participant was asked to select the top two results that best matched the
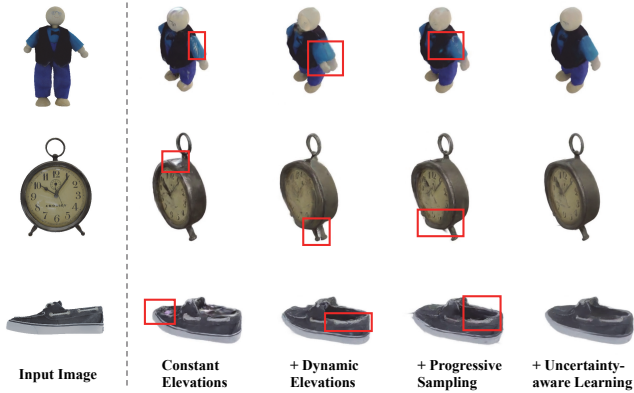
Figure 5. **Ablation analysis on the impact of progressive sampling and uncertainty-aware learning.** These techniques effectively mitigate artifacts, floats, and geometric deformations in inconsistent regions, resulting in visually enhanced 3D assets.
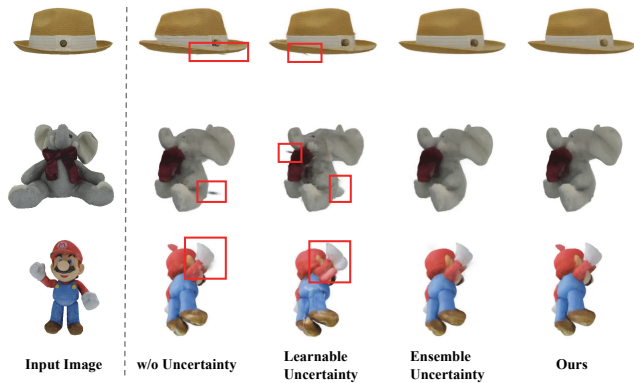

Figure 6. **Ablation analysis of the uncertainty estimation design.** Our method models uncertainty through the absolute difference between two concurrently optimized Gaussian models, providing stability and efficiency.

Figure 7. **Ablation analysis of the uncertainty weight** λ. Increasing λ reduces artifacts, but may make the generated results may become smoother and blurrier. In our experiments, $\lambda = 5$ achieves the optimal balance.

Figure 8. **Impact of Perturbed-Attention Guidance (PAG)** [1]. PAG enhances structural coherence and texture details, improving the visual quality across the generated multi-view frames. In this example, red bounding boxes highlight the quality improvements introduced by PAG in specific image regions.

input image and exhibited the highest visual quality, with the total preference score in the table summing to 200%. The collected preferences were then analyzed to compare the performance of our method with other state-of-the-art approaches. As shown in the results, our method was selected more frequently, demonstrating its ability to consistently produce the most visually compelling 3D assets.

4.2. Ablation Studies and Further Discussion

Impact of Progressive Sampling and Uncertainty-aware Learning. In typical two-stage methods, video frames with fixed elevations are generated and used as pseudo-labels to supervise the optimization of 3D assets. However, limited viewpoints often leave the top and bottom areas under-reconstructed, as shown in Figure 5. To address this limitation, we sample multiple videos from a wide range of viewpoints, improving coverage for top- and bottom-view
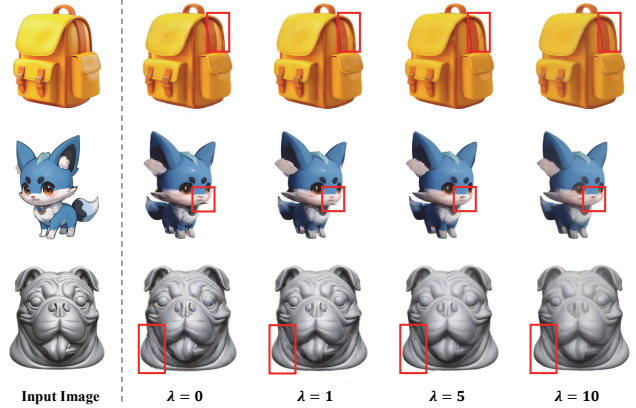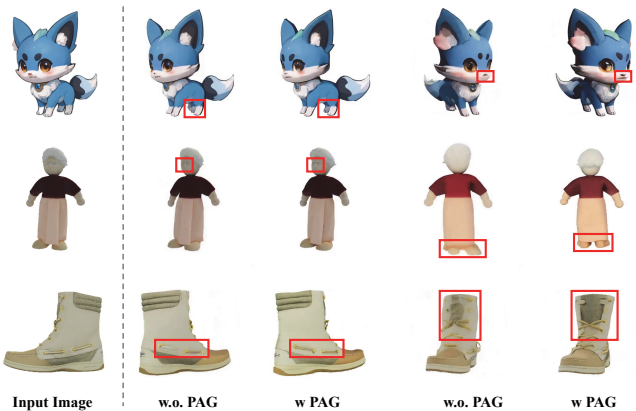
perspectives. Through progressive sampling, we start with a small number of frames to achieve an accurate initialization, and later refine texture details with the full set of frames, effectively preventing geometric deformations caused by initialization errors. Furthermore, uncertainty-aware learning dynamically identifies inconsistent regions in the pseudo-labels and adjust the supervision strength. Our approach effectively mitigates common issues such as artifacts and floats that often arise in prior works. By addressing these inconsistencies, our method ensures smoother and more accurate results, leading to visually improved 3D assets with better geometry and texture coherence.

Design of Uncertainty Estimation. We explore different approaches for uncertainty estimation, as shown in Figure 6. Assigning a learnable variance property to 3DGS [19]

results in poorer performance in some cases, likely due to training instability caused by directly regressing uncertainty. In contrast, the ensemble approach simultaneously optimizes multiple Gaussian models, averaging their predictions to generate the rendered image, with variance serving as a measure of uncertainty. This approach effectively alleviated noise, artifacts, and floats at the edges of generated 3D assets, resulting in a smoother output. Our method can be seen as a simplified ensemble approach. Experimental results show that two Gaussian models are sufficient, and their absolute difference accurately modeling uncertainty, producing similar benefits with greater efficiency.

Impact of the Uncertainty Weight λ. We conduct an ablation study to assess the impact of the uncertainty weight λ, as shown in Figure 7. When λ is set to a low value, the pixel-wise weights in uncertainty regularization become uniform, failing to differentiate between inconsistent and consistent regions. This results in insufficient mitigation of artifacts and floats arising from over-reconstruction in inconsistent regions. In contrast, a high value for λ substantially reduces supervision in high-uncertainty regions, effectively alleviating artifacts and floats but may lead to under-reconstruction, where inconsistent areas become overly smooth and blurry. Our experiments show that $\lambda = 5$ strikes an optimal balance, significantly reducing artifacts while preserving texture details and preventing excessive smoothing.

Impact of Perturbed-Attention Guidance (PAG). In our approach, we employ SV3D [55] to generate frames across a wide range of viewpoints. However, some generated samples exhibit distorted geometry or blurred textures. To address these issues, we integrate PAG [1] into SV3D, which enhances generation quality by guiding the denoising process away from the artificially degraded samples. As shown in Figure 8, the pseudo labels generated with PAG exhibit improved structure integrity and clearer, sharper textures.

5. Conclusion

In this work, we present a novel approach for Image-to-3D generation by incorporating uncertainty-aware learning. Our contributions are twofold: (1) we model pseudo-labels uncertainty by capturing the stochastic differences between two concurrently optimized Gaussian models; and (2) we apply uncertainty regularization, dynamically adjusting pixel-wise loss weights based on the estimated uncertainty map. This approach effectively mitigates conflicts within the generated pseudo-frames. By dynamically detecting inconsistencies among pseudo-labels during optimization process, our method significantly reduces artifacts and floats along the edges of the 3D assets, resulting in smoother and more accurate outputs. Extensive experiments demonstrate the effectiveness of our approach in enhancing the visual quality of 3D generation.

References

[1] Donghoon Ahn, Hyoungwon Cho, Jaewon Min, Wooseok Jang, Jungwoo Kim, SeonHwa Kim, Hyun Hee Park, Kyong Hwan Jin, and Seungryong Kim. Self-rectifying diffusion sampling with perturbed-attention guidance. *arXiv:2403.17377*, 2024. 6, 8, 9

[2] Andreas Blattmann, Tim Dockhorn, Sumith Kulal, Daniel Mendelevitch, Maciej Kilian, Dominik Lorenz, Yam Levi, Zion English, Vikram Voleti, Adam Letts, et al. Stable video diffusion: Scaling latent video diffusion models to large datasets. *arXiv:2311.15127*, 2023. 2, 4

[3] Andreas Blattmann, Robin Rombach, Huan Ling, Tim Dockhorn, Seung Wook Kim, Sanja Fidler, and Karsten Kreis. Align your latents: High-resolution video synthesis with latent diffusion models. In *CVPR*, 2023. 4

[4] Mark Boss, Zixuan Huang, Aaryaman Vasishta, and Varun Jampani. Sf3d: Stable fast 3d mesh reconstruction with uv-unwrapping and illumination disentanglement. *arXiv:2408.00653*, 2024. 3

[5] Yiyang Chen, Zhedong Zheng, Wei Ji, Leigang Qu, and Tat-Seng Chua. Composed image retrieval with text feedback via multi-grained uncertainty regularization. In *ICLR*, 2024. 3

[6] Zilong Chen, Yikai Wang, Feng Wang, Zhengyi Wang, and Huaping Liu. V3d: Video diffusion models are effective 3d generators. *arXiv:2403.06738*, 2024. 2, 3, 6, 7

[7] Laura Downs, Anthony Francis, Nate Koenig, Brandon Kinman, Ryan Hickman, Krista Reymann, Thomas B McHugh, and Vincent Vanhoucke. Google scanned objects: A high-quality dataset of 3d scanned household items. In *ICRA*, 2022. 6

[8] Shivam Duggal and Deepak Pathak. Topologically-aware deformation fields for single-view 3d reconstruction. In *CVPR*, 2022. 2

[9] Yarin Gal and Zoubin Ghahramani. Dropout as a bayesian approximation: Representing model uncertainty in deep learning. In *ICML*, 2016. 3

[10] Lily Goli, Cody Reading, Silvia Sellán, Alec Jacobson, and Andrea Tagliasacchi. Bayes' rays: Uncertainty quantification for neural radiance fields. In *CVPR*, 2024. 3

[11] Anchit Gupta, Wenhan Xiong, Yixin Nie, Ian Jones, and Barlas Oğuz. 3dgen: Triplane latent diffusion for textured mesh generation. *arXiv:2303.05371*, 2023. 2

[12] Jonathan Ho, Ajay Jain, and Pieter Abbeel. Denoising diffusion probabilistic models. In *NeurIPS*, 2020. 4

[13] Yicong Hong, Kai Zhang, Jiuxiang Gu, Sai Bi, Yang Zhou, Difan Liu, Feng Liu, Kalyan Sunkavalli, Trung Bui, and Hao Tan. LRM: large reconstruction model for single image to 3d. In *ICLR*, 2024. 3

[14] Wen Jiang, Boshu Lei, and Kostas Daniilidis. Fisherrf: Active view selection and uncertainty quantification for radiance fields using fisher information. *arXiv:2311.17874*, 2023. 3

[15] Liren Jin, Xieyuanli Chen, Julius Rückin, and Marija Popović. Neu-nbv: Next best view planning using uncertainty estimation in image-based neural rendering. In *IROS*, 2023. 3

[16] Heewoo Jun and Alex Nichol. Shap-e: Generating conditional 3d implicit functions. *arXiv:2305.02463*, 2023. 2

[17] Tero Karras, Miika Aittala, Timo Aila, and Samuli Laine. Elucidating the design space of diffusion-based generative models. In *NeurIPS*, 2022. 4

[18] Alex Kendall and Yarin Gal. What uncertainties do we need in bayesian deep learning for computer vision? In *NeurIPS*, 2017. 3

[19] Bernhard Kerbl, Georgios Kopanas, Thomas Leimkühler, and George Drettakis. 3d gaussian splatting for real-time radiance field rendering. *ACM Trans. Graph.*, 2023. 2, 3, 6, 8

[20] Durk P Kingma, Tim Salimans, and Max Welling. Variational dropout and the local reparameterization trick. In *NeurIPS*, 2015. 3

[21] Marcus Klasson, Riccardo Mereu, Juho Kannala, and Arno Solin. Sources of uncertainty in 3d scene reconstruction. *arXiv:2409.06407*, 2024. 3

[22] Jinsol Lee and Ghassan AlRegib. Gradients as a measure of uncertainty in neural networks. In *ICIP*, 2020. 3

[23] Monica MQ Li, Pierre-Yves Lajoie, and Giovanni Beltrame. Frequency-based view selection in gaussian splatting reconstruction. *arXiv:2409.16470*, 2024. 3

[24] Peng Li, Yuan Liu, Xiaoxiao Long, Feihu Zhang, Cheng Lin, Mengfei Li, Xingqun Qi, Shanghang Zhang, Wenhan Luo, Ping Tan, et al. Era3d: High-resolution multiview diffusion using efficient row-wise attention. *arXiv:2405.11616*, 2024. 2, 3

[25] Mattia Litrico, Alessio Del Bue, and Pietro Morerio. Guiding pseudo-labels with uncertainty estimation for source-free unsupervised domain adaptation. In *CVPR*, 2023. 3

[26] Minghua Liu, Chao Xu, Haian Jin, Linghao Chen, Mukund Varma T, Zexiang Xu, and Hao Su. One-2-3-45: Any single image to 3d mesh in 45 seconds without per-shape optimization. In *NeurIPS*, 2024. 2

[27] Ruoshi Liu, Rundi Wu, Basile Van Hoorick, Pavel Tokmakov, Sergey Zakharov, and Carl Vondrick. Zero-1-to-3: Zero-shot one image to 3d object. In *ICCV*, 2023. 2, 6

[28] Yuan Liu, Cheng Lin, Zijiao Zeng, Xiaoxiao Long, Lingjie Liu, Taku Komura, and Wenping Wang. Syncdreamer: Generating multiview-consistent images from a single-view image. In *ICLR*, 2024. 2, 3

[29] Ricardo Martin-Brualla, Noha Radwan, Mehdi SM Sajjadi, Jonathan T Barron, Alexey Dosovitskiy, and Daniel Duckworth. Nerf in the wild: Neural radiance fields for unconstrained photo collections. In *CVPR*, 2021. 3

[30] Luke Melas-Kyriazi, Iro Laina, Christian Rupprecht, Natalia Neverova, Andrea Vedaldi, Oran Gafni, and Filippos Kokkinos. IM-3D: iterative multiview diffusion and reconstruction for high-quality 3d generation. In *ICML*, 2024. 2, 3

[31] Lars Mescheder, Michael Oechsle, Michael Niemeyer, Sebastian Nowozin, and Andreas Geiger. Occupancy networks: Learning 3d reconstruction in function space. In *CVPR*, 2019. 2

[32] Jay Nandy, Wynne Hsu, and Mong Li Lee. Towards maximizing the representation gap between in-domain & out-of-distribution examples. In *NeurIPS*, 2020. 3

[33] Radford M Neal. *Bayesian learning for neural networks*. Springer Science & Business Media, 2012. 3

[34] Alex Nichol, Heewoo Jun, Prafulla Dhariwal, Pamela Mishkin, and Mark Chen. Point-e: A system for generating 3d point clouds from complex prompts. *arXiv:2212.08751*, 2022. 2

[35] Xuran Pan, Zihang Lai, Shiji Song, and Gao Huang. Activenerf: Learning where to see with uncertainty estimation. In *ECCV*, 2022. 3

[36] Simon Parsons. Bayesian networks and decision graphs. *Springer*, 23(4), 2008. 3

[37] Ben Poole, Ajay Jain, Jonathan T. Barron, and Ben Mildenhall. Dreamfusion: Text-to-3d using 2d diffusion. In *ICLR*, 2023. 2

[38] Guocheng Qian, Jinjie Mai, Abdullah Hamdi, Jian Ren, Aliaksandr Siarohin, Bing Li, Hsin-Ying Lee, Ivan Skorokhodov, Peter Wonka, Sergey Tulyakov, and Bernard Ghanem. Magic123: One image to high-quality 3d object generation using both 2d and 3d diffusion priors. In *ICLR*, 2024. 2

[39] Maithra Raghu, Katy Blumer, Rory Sayres, Ziad Obermeyer, Bobby Kleinberg, Sendhil Mullainathan, and Jon Kleinberg. Direct uncertainty prediction for medical second opinions. In *ICML*, 2019. 3

[40] Robin Rombach, Andreas Blattmann, Dominik Lorenz, Patrick Esser, and Björn Ommer. High-resolution image synthesis with latent diffusion models. In *CVPR*, 2022. 2, 4

[41] Sara Sabour, Suhani Vora, Daniel Duckworth, Ivan Krasin, David J Fleet, and Andrea Tagliasacchi. Robustnerf: Ignoring distractors with robust losses. In *CVPR*, 2023. 3

[42] Chitwan Saharia, William Chan, Saurabh Saxena, Lala Li, Jay Whang, Emily L Denton, Kamyar Ghasemipour, Raphael Gontijo Lopes, Burcu Karagol Ayan, Tim Salimans, et al. Photorealistic text-to-image diffusion models with deep language understanding. In *NeurIPS*, 2022. 2

[43] Luca Savant, Diego Valsesia, and Enrico Magli. Modeling uncertainty for gaussian splatting. *arXiv:2403.18476*, 2024. 3

[44] Jianxiong Shen, Adria Ruiz, Antonio Agudo, and Francesc Moreno-Noguer. Stochastic neural radiance fields: Quantifying uncertainty in implicit 3d representations. In *3DV*, 2021. 3

[45] Jianxiong Shen, Antonio Agudo, Francesc Moreno-Noguer, and Adria Ruiz. Conditional-flow nerf: Accurate 3d modelling with reliable uncertainty quantification. In *ECCV*, 2022. 3

[46] Ruoxi Shi, Hansheng Chen, Zhuoyang Zhang, Minghua Liu, Chao Xu, Xinyue Wei, Linghao Chen, Chong Zeng, and Hao Su. Zero123++: a single image to consistent multi-view diffusion base model. *arXiv:2310.15110*, 2023. 2, 3

[47] Yichun Shi, Peng Wang, Jianglong Ye, Long Mai, Kejie Li, and Xiao Yang. Mvdream: Multi-view diffusion for 3d generation. In *ICLR*, 2024. 2, 3

[48] Jiaming Song, Chenlin Meng, and Stefano Ermon. Denoising diffusion implicit models. In *ICLR*, 2021. 4

[49] Matthew Strong, Boshu Lei, Aiden Swann, Wen Jiang, Kostas Daniilidis, and Monroe Kennedy III. Next best sense:

Guiding vision and touch with fisherrf for 3d gaussian splatting. *arXiv:2410.04680*, 2024. 3

[50] Wei Sun, Qi Zhang, Yanzhao Zhou, Qixiang Ye, Jianbin Jiao, and Yuan Li. Uncertainty-guided optimal transport in depth supervised sparse-view 3d gaussian. *arXiv:2405.19657*, 2024. 3

[51] Jiaxiang Tang, Jiawei Ren, Hang Zhou, Ziwei Liu, and Gang Zeng. Dreamgaussian: Generative gaussian splatting for efficient 3d content creation. In *ICLR*, 2024. 6, 7

[52] Jiaxiang Tang, Zhaoxi Chen, Xiaokang Chen, Tengfei Wang, Gang Zeng, and Ziwei Liu. Lgm: Large multi-view gaussian model for high-resolution 3d content creation. In *ECCV*, 2025. 6, 7

[53] Dmitry Tochilkin, David Pankratz, Zexiang Liu, Zixuan Huang, Adam Letts, Yangguang Li, Ding Liang, Christian Laforte, Varun Jampani, and Yan-Pei Cao. Triposr: Fast 3d object reconstruction from a single image. *arXiv:2403.02151*, 2024. 3

[54] Alex Trevithick and Bo Yang. Grf: Learning a general radiance field for 3d representation and rendering. In *ICCV*, 2021. 2

[55] Vikram Voleti, Chun-Han Yao, Mark Boss, Adam Letts, David Pankratz, Dmitry Tochilkin, Christian Laforte, Robin Rombach, and Varun Jampani. Sv3d: Novel multi-view synthesis and 3d generation from a single image using latent video diffusion. In *ECCV*, 2025. 2, 3, 4, 6, 9

[56] Nanyang Wang, Yinda Zhang, Zhuwen Li, Yanwei Fu, Wei Liu, and Yu-Gang Jiang. Pixel2mesh: Generating 3d mesh models from single rgb images. In *ECCV*, 2018. 2

[57] Peng Wang and Yichun Shi. Imagedream: Image-prompt multi-view diffusion for 3d generation. *arXiv:2312.02201*, 2023. 2, 3

[58] Tengfei Wang, Bo Zhang, Ting Zhang, Shuyang Gu, Jianmin Bao, Tadas Baltrusaitis, Jingjing Shen, Dong Chen, Fang Wen, Qifeng Chen, et al. Rodin: A generative model for sculpting 3d digital avatars using diffusion. In *CVPR*, 2023. 2

[59] Zhou Wang, Alan C Bovik, Hamid R Sheikh, and Eero P Simoncelli. Image quality assessment: from error visibility to structural similarity. *IEEE Transactions on Image Processing*, 2004. 5

[60] Sangmin Woo, Byeongjun Park, Hyojun Go, Jin-Young Kim, and Changick Kim. Harmonyview: Harmonizing consistency and diversity in one-image-to-3d. In *CVPR*, 2024. 2, 3

[61] Shuang Wu, Youtian Lin, Feihu Zhang, Yifei Zeng, Jingxi Xu, Philip Torr, Xun Cao, and Yao Yao. Direct3d: Scalable image-to-3d generation via 3d latent diffusion transformer. *arXiv:2405.14832*, 2024. 2

[62] Dongyu Yan, Jianheng Liu, Fengyu Quan, Haoyao Chen, and Mengmeng Fu. Active implicit object reconstruction using uncertainty-guided next-best-view optimization. *IEEE Robotics and Automation Letters*, 2023. 3

[63] Haibo Yang, Yang Chen, Yingwei Pan, Ting Yao, Zhineng Chen, Chong-Wah Ngo, and Tao Mei. Hi3d: Pursuing high-resolution image-to-3d generation with video diffusion models. In *ACM MM*, 2024. 2, 3, 6, 7

[64] Shuzhou Yang, Yu Wang, Haijie Li, Jiarui Meng, Xiandong Meng, and Jian Zhang. Fourier123: One image to high-quality 3d object generation with hybrid fourier score distillation. *arXiv:2405.20669*, 2024. 2

[65] Han Yi, Zhedong Zheng, Xiangyu Xu, and Tat-seng Chua. Progressive text-to-3d generation for automatic 3d prototyping. *arXiv:2309.14600*, 2023. 3

[66] Tianyuan Yu, Da Li, Yongxin Yang, Timothy M Hospedales, and Tao Xiang. Robust person re-identification by modelling feature uncertainty. In *ICCV*, 2019. 3

[67] Huangying Zhan, Jiyang Zheng, Yi Xu, Ian Reid, and Hamid Rezatofighi. Activermap: Radiance field for active mapping and planning. *arXiv:2211.12656*, 2022. 3

[68] Richard Zhang, Phillip Isola, Alexei A Efros, Eli Shechtman, and Oliver Wang. The unreasonable effectiveness of deep features as a perceptual metric. In *CVPR*, 2018. 5

[69] Ruiyang Zhang, Hu Zhang, Hang Yu, and Zhedong Zheng. Harnessing uncertainty-aware bounding boxes for unsupervised 3d object detection. *arXiv:2408.00619*, 2024. 3

[70] Saining Zhang, Baijun Ye, Xiaoxue Chen, Yuantao Chen, Zongzheng Zhang, Cheng Peng, Yongliang Shi, and Hao Zhao. Drone-assisted road gaussian splatting with cross-view uncertainty. *arXiv:2408.15242*, 2024. 3

[71] Xuanmeng Zhang, Zhedong Zheng, Daiheng Gao, Bang Zhang, Yi Yang, and Tat-Seng Chua. Multi-view consistent generative adversarial networks for compositional 3d-aware image synthesis. *International Journal of Computer Vision*, 131(8), 2023. 2

[72] Zhedong Zheng and Yi Yang. Rectifying pseudo label learning via uncertainty estimation for domain adaptive semantic segmentation. *International Journal of Computer Vision*, 2021. 3

[73] Zi-Xin Zou, Zhipeng Yu, Yuan-Chen Guo, Yangguang Li, Ding Liang, Yan-Pei Cao, and Song-Hai Zhang. Triplane meets gaussian splatting: Fast and generalizable single-view 3d reconstruction with transformers. In *CVPR*, 2024. 6, 7

[74] Qi Zuo, Xiaodong Gu, Lingteng Qiu, Yuan Dong, Zhengyi Zhao, Weihao Yuan, Rui Peng, Siyu Zhu, Zilong Dong, Liefeng Bo, et al. Videomv: Consistent multi-view generation based on large video generative model. *arXiv:2403.12010*, 2024. 2, 3